U-Net for Efficient Liver Segmentation from 3D CT Data

Boonnatee Sakboonyarat and Pinyo Taeprasartsit

April 9, 2018

U-Net for Efficient Liver Segmentation from 3D CT Data

***Abstract*— In order to diagnosis the liver cancer in early stage, the liver segmentation technique for image processing had been challenged by the non-homogeneous Hounsfield Unit (HU) of nearby area around the liver in 3D computed tomography image (CT image) and the similar morphological shape of nearby organ. The previous study reported the high accuracy and precision segmentations by using hybrid method, (combining image-based and model-based method). In order to reduce the processing time of segmentation, this U-Net model was developed by using the training dataset (16 images) and testing dataset (4 images) from the Segmentation of the Liver 2007 (SLIVER07). The results showed the high accuracy segmentation operated under 0.02 seconds per slice.**

Keywords—liver segmentation, U-Net, 3D CT Data

I. INTRODUCTION

In 2012, GLOBOCAN reported 8.2 million deaths and 14.1 million new cancer cases worldwide [1]. In developed countries, such as Thailand, the liver cancer was the leading cause of cancer death. In order to reduce the risk of cancer death, the abdominal computed tomography (CT) images were examined and diagnosed in early stage patients.

To produce the abdominal CT-images, the radiographic tube emits the X-rays in cross-sectional direction to the target organs. While rotating around patient, the narrow fan beam was emitted, transmitted though the patients, and entered the array of detectors on opposite side. Due to the non-homogeneous density of patient body that X-rays transmitted, the different amount of X-rays were detected and represented in Housefield Unit (HU). Nowadays, the most of CT-Scan machines are multi-slice CT (MSCT, Figure 1), which is developed from single-slice CT (SSCT) by increase the rows of detector array (4, 8, 16, 24, 32, 64, 128, 256, 320 slices)[2],[3, pp. 6–10]. Consequently, MSCT machine had capacity to record the multiple images in one scanning shot leading to product the high resolution images and significantly reduce the total operating time to scan.

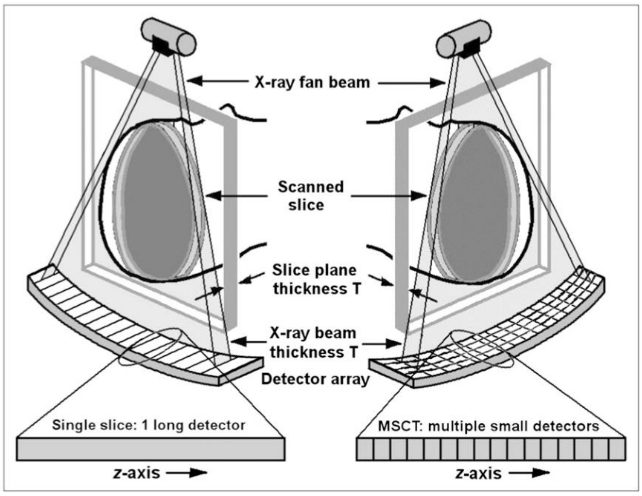

Figure 1. (Left) SSCT arrays containing single, long elements along z-axis. (Right) MSCT arrays with several rows of small detector elements. [4, pp. 57–68]

However, the current diagnosis of liver cancer with Computed Tomogram (TC-Scan) was time-consuming process due to the size of image and complexity of organ images around the liver. The organ photography contained the three-dimension (3D) data with size of N × 512 × 512, where N is the resolution of scanning in millimeter. The high resolution TC-Scan image required longer time and amount of computing resources to process. Furthermore, the abdominal CT-Images possibly contain the nearby organ in abdominal cavity, such as liver, kidney, and spleen. These organs have overlapped range of Housefield Unit (HU) (Table 1) and difficult to segmenting and clustering with image processing techniques.

The rest of this article is organized as follows: Section II explains the base of this research from some studies related to segmentation of the liver from CT-Images and method to segment the object from background images. Section III Introduces the description of our U-Net Model for Efficient Liver Segmentation method. Section IV presents the experiment process and results of our method. Finally, Section V, conclusions the article.

TABLE I Hounsfield numbers for selected tissues

Tissue	HU Value
Air	-1000
Lung parenchyma	-910 to -850
Fat	-70 to -110
Water	0
Kidneys	27 to 30
Pancreas	20 to 30
Brain	35
Muscles	40
Liver	45 to 65
Spleen	50
Fresh blood in the brain	65
Bone	1,300

II. RELATED WORK

In 2007, the Medical Image Computing and Computer Assisted Intervention Society (MICCAI Society) initiated Segmentation of the Liver 2007 (SLIVER07) competition [5]. The research competitor teams received CT-images set for training (20 images) and testing (10 images) and used the five criteria, which were Volumetric Overlap Error (VOE), Relative Volume Difference (RVD), Average Symmetric Surface Distance (ASSD), Root Mean Square Symmetric Surface Distance (RMSD) and Maximum Symmetric Surface Distance (MSSD) [6]–[8], for evaluate the accuracy and precision.

Since the SLIVER in 2007, the number of researches about segmentation of the liver from CT-Images had published. Chen et al. (2012) classified the method to segment the object from background image into three groups [9]:

1) Image based method that used image processing technique with raw data in CT-image, such as thresholding extraction, region growing [10], [11], Morphological operations [12], Active contours [13], [14], Live wire[15], [16], Watershed [17], Fuzzy connectedness [18], Graph Cuts[19]–[21]. These methods required the high quality of CT-images to archive high accuracy and precision.

2) Model based method that used the synthetic statistical models, such as statistical active shape modes [22]–[25], statistical active appearance models [26], [27]. These methods did not require the high quality CT-image, but required a number of CT-images instead.

3) Hybrid method that combined the image based method and model based method [9], [28]–[30].

The recent researches of CT-image segmentation for liver cancer had been reported by using the hybrid method. In order to practical use in clinics, this study is trying to reduce the long image processing by finding an optimized modeling template for use the hybrid methods with parallel processing. This U-Net Model for Efficient Liver Segmentation from 3D CT Data is developed by training data set to find the best template that can learn the value of HU and the shape of liver.

III. MATERIALS AND METHODOLOGY

A. *Data Preparation*

Our test dataset comprised 20 CT from the database of 3D Segmentation in the Clinic: A Grand Challenge Liver 2007 (SLIVER07) competition, as summarized in Table I and Group CT Image for training and testing set data from 20 CT original as summarized in Table III and Table IV

TABLE II

Description for 20 CT Image

			HU Values + 1024 of Liver Segmentation		
ID	Number of Slices	Resolution (mm)	Begin Value	End Value	Mean0 Value
L01	183	0.742 x 0.742 x 1.500	929	1223	1110
L02	127	0.628 x 0.628 x 3.000	903	1257	1116
L03	159	0.759 x 0.759 x 3.000	970	1304	1126
L04	143	0.709 x 0.709 x 1.000	990	1453	1207
L05	215	0.576 x 0.576 x 1.000	1010	1346	1158
L06	147	0.669 x 0.669 x 2.000	1032	1281	1170
L07	167	0.812 x 0.812 x 1.000	956	1315	1122
L08	151	0.664 x 0.664 x 1.000	922	1380	1131
L09	139	0.746 x 0.746 x 1.000	1030	1391	1192
L10	127	0.585 x 0.585 x 1.000	1017	1434	1197
L11	259	0.585 x 0.585 x 1.000	1017	1321	1168
L12	147	0.699 x 0.699 x 1.000	982	1335	1160
L13	123	0.703 x 0.703 x 1.250	992	1236	1135
L14	431	0.718 x 0.718 x 5.000	905	1183	1116
L15	263	0.585 x 0.585 x 1.000	968	1391	1179
L16	151	0.742 x 0.742 x 1.500	925	1256	1124
L17	163	0.683 x 0.683 x 2.000	956	1275	1157
L18	163	0.740 x 0.740 x 1.000	924	1388	1163
L19	159	0.611 x 0.611 x 0.700	957	1347	1164
L20	307	0.703 x 0.703 x 2.500	950	1229	1148

TABLE III

Group CT Image

Group CT Image By ID				
G1	G2	G3	G4	G5
L01	L02	L03	L04	L05
L06	L07	L08	L09	L10
L11	L12	L13	L14	L15
L16	L17	L18	L19	L20

TABLE IV

Group training and testing set data

ID	Training Set		Testing Set	
	Group	Number of Slices	Group	Number of Slices
T1	G2,G3,G4,G5	2,984.00	G1	740
T2	G1,G3,G4,G6	3,120.00	G2	604
T3	G1,G2,G4,G7	3,128.00	G3	596
T4	G1,G2,G3,G8	2,995.00	G4	729
T5	G1,G2,G3,G5	2,812.00	G5	912

B. *U-Net*

The U-Net is convolutional network architecture for fast and precise segmentation of images [31], This is that process copying low-level properties to the corresponding high level, it actually creates a path for dissemination of information that allows the signal to spread between low and high levels more easily, which not only facilitates backward propagation during training sessions, but also compensates low-level finer details to high-level semantic features. In this article, utilize U-Net architecture is illustrated in Figure 2. It consists of a contractive path on the left and an extensive path on the right.

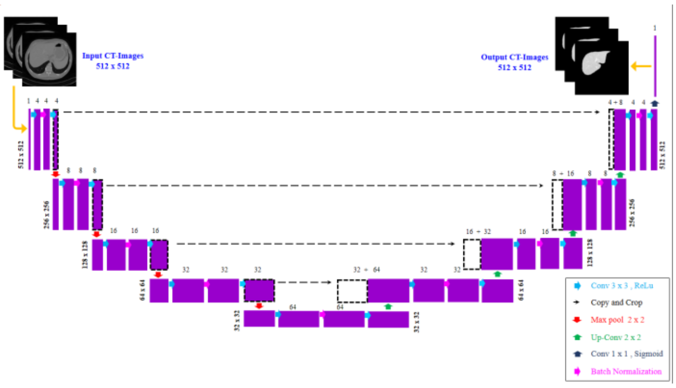

Figure 2. The fully CNN called U-Net

The U-Net architecture include input layer, convolutional layer, pooling layer, up sampling layer and output layer. In this work propose loss function based on dice coefficient, which is a quantity ranging between 0 and 1 which we aim to maximise.

IV. EXPERRIMENTS

To demonstrate the accuracy and effectiveness of the proposed format as discussed below.

A. Preprocessing Histograms

The proposed algorithm is the preprocessing histograms of intensity distributions of abdominal computed tomography images. Uses three functions for normalization data as follows:

$$P(x;\mu,\sigma,\alpha) = e^{-\frac{1}{2}\left(\frac{x-\mu}{\alpha\cdot\sigma}\right)} \tag{1}$$

$$C(x;\mu,\sigma,\alpha) = \frac{1}{2}\left[1 + erf\left(\frac{x-\mu}{\alpha\cdot\sigma\sqrt{2}}\right)\right] \tag{2}$$

$$M(x;\mu,\sigma,\alpha) = \begin{cases} \frac{1}{2}\left[1 + erf\left(\frac{x-(\mu-\alpha\cdot\sigma)}{\alpha\cdot\sigma\sqrt{2}}\right)\right], & x-(\mu+3\alpha\cdot\sigma) : \\ 0, & x-(\mu+3\alpha\cdot\sigma) \end{cases} \tag{3}$$

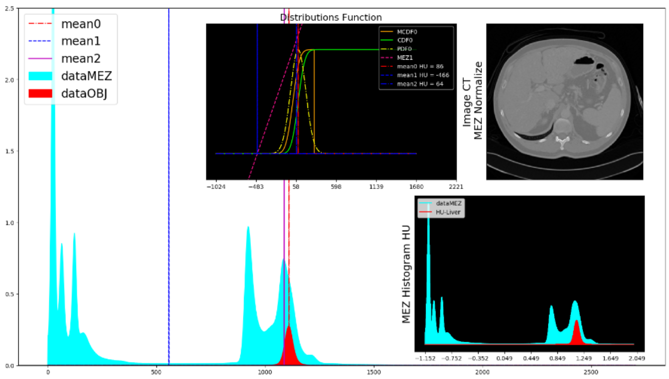

B. Evaluation Metrics

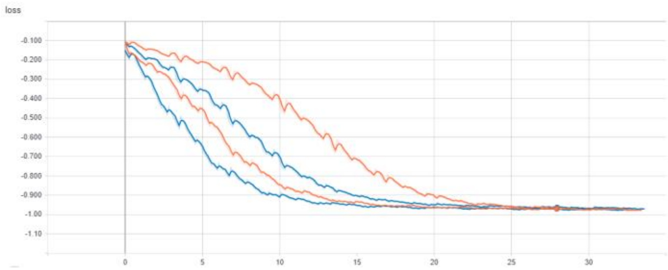

C. Comparisons

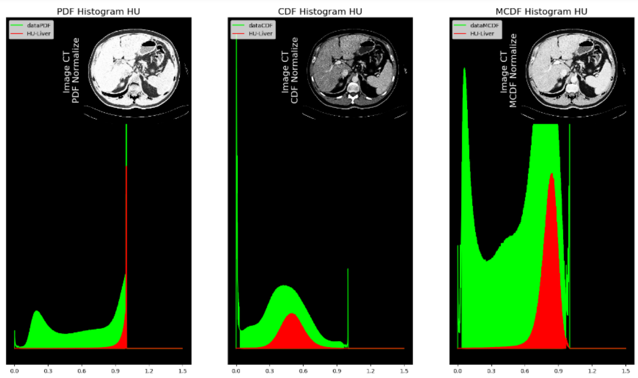

V. CONCLUSION

The U-Net model for efficient liver segmentation was developed by using dataset from the Segmentation of the Liver 2007 (SLIVER07) competition. The 123,689 parameters in U-Net model were trained with sixteen datasets and tested with four datasets. The results showed that this novel U-Net model had capacity to archive high accuracy segmentation with the average processing time of 0.02 seconds per slice.

ACKNOWLEDGMENT

We would like to thank the SLIVER07 for CT images used in the experiments.

REFERENCES

[1] L. A. Torre, F. Bray, R. L. Siegel, J. Ferlay, J. Lortet-Tieulent, and A. Jemal, “Global cancer statistics, 2012,” *CA: A Cancer Journal for Clinicians*, vol. 65, no. 2, pp. 87–108, 2015.

[2] Robert Cierniak, *X-RAY COMPUTED TOMOGRAPHY IN BIOMEDICAL ENGINEERING*, vol. 2011. Springer London.

[3] *Multislice CT*, 3rd ed. Springer Berlin Heidelberg, 2009.

[4] L. W. Goldman, “Principles of CT: Multislice CT,” *Journal of Nuclear Medicine Technology*, vol. 36, no. 2, pp. 57–68, 2008.

[5] T. Heimann, M. Styner, and B. van Ginneken, “Sliver07(2007),” Aug-2013. [Online]. Available: http://www.sliver07.org.

[6] T. Heimann, B. van Ginneken, and M. A. Styner, “Comparison and Evaluation of Methods for Liver

Segmentation From CT Datasets," *Medical Imaging, IEEE Transactions on*, vol. 28, no. 8, pp. 1251–1265, Aug. 2009.

[7] P. Jaccard, *Etude comparative de la distribution florale dans une portion des Alpes et du Jura*, vol. 37. Impr. Corbaz, 1901.

[8] S. Arya, D. M. Mount, N. S. Netanyahu, R. Silverman, and A. Y. Wu, "An Optimal Algorithm for Approximate Nearest Neighbor Searching Fixed Dimensions," *J. ACM*, vol. 45, no. 6, pp. 891–923, Nov. 1998.

[9] X. Chen, J. K. Udupa, U. Bagci, Y. Zhuge, and J. Yao, "Medical Image Segmentation by Combining Graph Cuts and Oriented Active Appearance Models," *IEEE Transactions on Image Processing*, vol. 21, no. 4, pp. 2035–2046, Apr. 2012.

[10] O. Gloger, J. Kühn, A. Stanski, H. Völzke, and R. Puls, "A fully automatic three-step liver segmentation method on LDA-based probability maps for multiple contrast MR images," *Magnetic Resonance Imaging*, vol. 28, no. 6, pp. 882–897, Jul. 2010.

[11] L. Rusk?, G. Bekes, G. N?meth, and M. Fidrich, *Fully automatic liver segmentation for contrast-enhanced CT images*. .

[12] H. Fujimoto, L. Gu, and T. Kaneko, "Recognition of abdominal organs using 3D mathematical morphology," *Systems and Computers in Japan*, vol. 33, no. 8, pp. 75–83, 2002.

[13] M. Kass, A. Witkin, and D. Terzopoulos, "Snakes: Active contour models," *International Journal of Computer Vision*, vol. 1, no. 4, pp. 321–331.

[14] F. Liu, B. Zhao, P. K. Kijewski, L. Wang, and L. H. Schwartz, "Liver segmentation for CT images using GVF snake," *Medical Physics*, vol. 32, no. 12, pp. 3699–3706, 2005.

[15] R. Malladi, J. A. Sethian, and B. C. Vemuri, "Shape modeling with front propagation: a level set approach," *IEEE Transactions on Pattern Analysis and Machine Intelligence*, vol. 17, no. 2, pp. 158–175, Feb. 1995.

[16] A. X. Falcão, J. K. Udupa, S. Samarasekera, S. Sharma, B. E. Hirsch, and R. de A. Lotufo, "User-Steered Image Segmentation Paradigms: Live Wire and Live Lane," *Graphical Models and Image Processing*, vol. 60, no. 4, pp. 233–260, Jul. 1998.

[17] H. Masoumi, A. Behrad, M. A. Pourmina, and A. Roosta, "Automatic liver segmentation in MRI images using an iterative watershed algorithm and artificial neural network," *Biomedical Signal Processing and Control*, vol. 7, no. 5, pp. 429–437, Sep. 2012.

[18] J. K. Udupa, P. K. Saha, and R. A. Lotufo, "Disclaimer: 'Relative fuzzy connectedness and object definition: theory, algorithms, and applications in image segmentation,'" *IEEE Transactions on Pattern Analysis and Machine Intelligence*, vol. 24, no. 11, p. I-1500, Nov. 2002.

[19] Y. Boykov and V. Kolmogorov, "An experimental comparison of min-cut/max- flow algorithms for energy minimization in vision," *IEEE Transactions on Pattern Analysis and Machine Intelligence*, vol. 26, no. 9, pp. 1124–1137, Sep. 2004.

[20] V. Kolmogorov and R. Zabin, "What energy functions can be minimized via graph cuts?," *IEEE Transactions on Pattern Analysis and Machine Intelligence*, vol. 26, no. 2, pp. 147–159, Feb. 2004.

[21] O. Veksler, "Star Shape Prior for Graph-Cut Image Segmentation," in *Computer Vision – ECCV 2008: 10th European Conference on Computer Vision, Marseille, France, October 12-18, 2008, Proceedings, Part III*, D. Forsyth, P. Torr, and A. Zisserman, Eds. Berlin, Heidelberg: Springer Berlin Heidelberg, 2008, pp. 454–467.

[22] T. F. Cootes, C. J. Taylor, D. H. Cooper, and J. Graham, "Active Shape Models-Their Training and Application," *Computer Vision and Image Understanding*, vol. 61, no. 1, pp. 38–59, Jan. 1995.

[23] A. F. Frangi, D. Rueckert, J. A. Schnabel, and W. J. Niessen, "Automatic construction of multiple-object three-dimensional statistical shape models: application to cardiac modeling," *IEEE Transactions on Medical Imaging*, vol. 21, no. 9, pp. 1151–1166, Sep. 2002.

[24] S. Seifert *et al.*, "Hierarchical parsing and semantic navigation of full body CT data," in *SPIE medical imaging*, 2009, pp. 725902–725902.

[25] H. Ling, S. K. Zhou, Y. Zheng, B. Georgescu, M. Suehling, and D. Comaniciu, "Hierarchical, learning-based automatic liver segmentation," in *Computer Vision and Pattern Recognition, 2008. CVPR 2008. IEEE Conference on*, 2008, pp. 1–8.

[26] T. F. Cootes, G. J. Edwards, and C. J. Taylor, "Active appearance models," *IEEE Transactions on Pattern Analysis and Machine Intelligence*, vol. 23, no. 6, pp. 681–685, Jun. 2001.

[27] M. B. Stegmann, B. K. Ersboll, and R. Larsen, "FAME-a flexible appearance modeling environment," *IEEE Transactions on Medical Imaging*, vol. 22, no. 10, pp. 1319–1331, Oct. 2003.

[28] C. Li *et al.*, "A Likelihood and Local Constraint Level Set Model for Liver Tumor Segmentation from CT Volumes," *IEEE Transactions on Biomedical Engineering*, vol. 60, no. 10, pp. 2967–2977, Oct. 2013.

[29] R. Wolz, C. Chu, K. Misawa, M. Fujiwara, K. Mori, and D. Rueckert, "Automated Abdominal Multi-Organ Segmentation With Subject-Specific Atlas Generation," *IEEE Transactions on Medical Imaging*, vol. 32, no. 9, pp. 1723–1730, Sep. 2013.

[30] G. Li, X. Chen, F. Shi, W. Zhu, J. Tian, and D. Xiang, "Automatic Liver Segmentation Based on Shape Constraints and Deformable Graph Cut in Ct Images," *IEEE Transactions on Image Processing*, vol. 24, no. 12, pp. 5315–5329, Dec. 2015.

[31] O. Ronneberger, P. Fischer, and T. Brox, "U-Net: Convolutional Networks for Biomedical Image Segmentation," in *Medical Image Computing and Computer-Assisted Intervention – MICCAI 2015*, Cham, 2015, pp. 234–241